Proceedings of the IASS-SLTE 2014 Symposium
"Shells, Membranes and Spatial Structures: Footprints"
15 to 19 September 2014, Brasilia, Brazil
Reyolando M.L.R.F. BRASIL and Ruy M.O. PAULETTI (eds.)

A Study on the Stretch Fabrication of Tensile Membrane Structures using ETFE Film

EulSeok JEONG*, Masaya KAWABATA[a]

*Research Engineer, Dept. of Architectural Engineering, Semyung University, Korea
65 Semyung-ro, Jecheon-si, Chungbuk, Korea, 390-711
jeong.eulseok.wx@gmail.com

[a] Associate Professor, Faculty of Engineering, Yokohama National University, Japan

Abstract

In this study, we confirm the possibility of applying stretch-fabrication on models with various shapes to allow technological establishment of such tensile film membrane structures, and shows through validation tests that this approach can be applied to actual structures. First, the applicability of stretch-fabrication is confirmed by introducing tension for study models with various shapes. Also, through validation tests, the effectiveness of the stretch-fabrication method using an arch and the viscous behavior of the film after stretch-fabrication is investigated. Additionally, the elasto-plastic analysis is carried out by considering the viscous behavior of film, and the validity of the analysis results is examined by comparing to experimental results. After stretch-fabrication, the mechanical behavior of the film is also investigated.

Keywords: ETFE film, membrane structure, stretch-fabrication, tension type, visco-plastic, elasto-plastic.

1. Introduction

Recently, Ethylene/TetraFluoroEthylene(ETFE) films have been used in numerous structures, such as greenhouses and stadiums, due to its greater transparency, weather resistance, and recyclability, etc., in comparison to existing membrane materials.

Most of the structural forms in which ETFE film is used are the cushion type (pneumatic membrane structures) and tension type (tensile membrane structures), which are generally accepted to be the most efficient forms.

Cushion type structures use the curvature of the membrane surface to reduce the stresses arising from additional loads, such as wind and snow. One of the features of this design is its ability to absorb the cushion rise induced creep strain resulting from the internal pressure. On the other hand, tension type structures are pulled outward from the exterior to introduce membrane tension. And such structures offer the advantage of a natural shape formed by tensile stress and eliminate the need for blast air.

Until recently, almost all ETFE film structures erected have been of the cushion type, but the number of tension type structures is currently increasing. But, there are problems of creep and relaxation of ETFE films under long-term stresses.

Also, membrane structures using the ETFE film are designed in two ways. One method is called "elastic design" and uses the first yield point as the allowable stress, the other method is called "elasto-plastic design" and uses a point in the plastic range as the allowable strength.

In a previous work, the authors proposed a method for stretching the film into the plastic region during initial tensioning as a way to increase its strength, and demonstrate its effectiveness(Kawabata *et al.* [1]). Two effects can be expected from stretching film. First, the yield point of the film is increased by strain hardening in the plastic region, thus allowing the user to increase the design strength. Second, crystallization is promoted by film elongation, which reduces creep and stress relaxation.

In this paper, we confirm the possibility of applying stretch-fabrication on models with various shapes to allow technological establishment of such tensile film membrane structures, and shows through validation tests that this approach can be applied to actual structures. First, the applicability of stretch-fabrication is confirmed by

introducing tension for study models with various shapes. Also, through validation tests, the effectiveness of the stretch-fabrication method using an arch and the viscous behavior of the film after stretch-fabrication is investigated. Additionally, the elasto-plastic analysis is carried out by considering the viscous behavior of film, and the validity of the analysis results is examined by comparing to experimental results. After stretch-fabrication, the mechanical behavior of the film is also investigated.

2. Case study

2.1 Introduction of study model

To verify the applicability of stretch fabrication to various shapes, five study models that differed in the position of the arch in the rectangular panel (Figure 1) were compared and reviewed.

The models were scaled to 1/5 of the actual size after members were examined. The actual panel dimensions were set as follows: a square frame of 3000 mm, arch height that is 15% of the span, and film thickness of 250 μm. The load conditions were set to consider long- and short-term loads (i.e., snow and wind) on the film. The members of the frame and arch were examined based on the analytical results of the film. Figure 2 shows the parallel arch model specimen accoding to the results of the parallel arch model. The member examination showed that the peripheral frame needed a steel cross-section with dimensions of L-150 mm × 75 mm × 9 mm × 12.5 mm, and the arch needed a steel pipe with dimensions of φ60.5 mm × 3.2 mm. Based on these results, study models were manufactured in square shapes with sides of 600 mm from a 50 μm thick ETFE film, L-30 mm × 30 mm × 2 mm × 600 mm angles for the peripheral frame, and φ13 mm × 1 mm aluminum pipe for the arch.

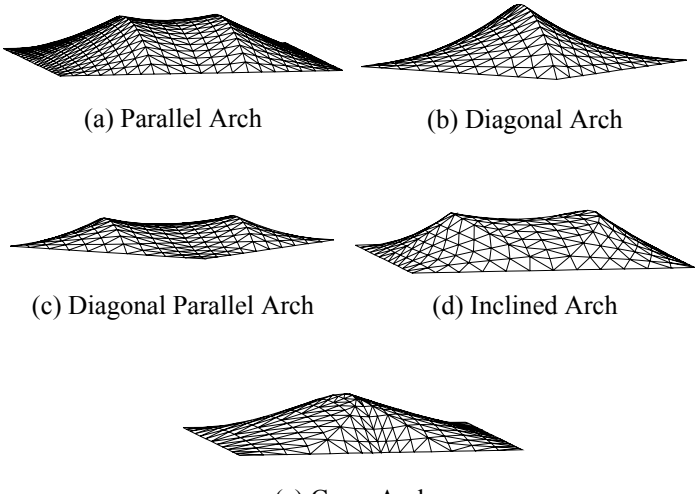

(a) Parallel Arch (b) Diagonal Arch

(c) Diagonal Parallel Arch (d) Inclined Arch

(e) Cross Arch

Figure 1: Classification of study model

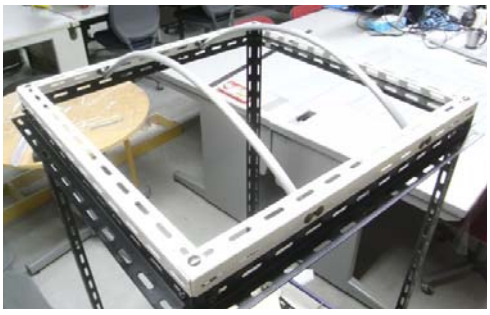

Figure 2: Test of study model

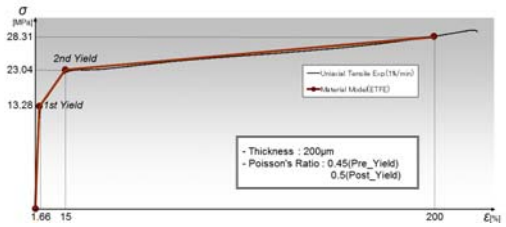

Figure 3: Material property of ETFE film

2.2 Shape finding of study model

The shape of each study model was determined in order to apply stretch fabrication to the model, and the cutting pattern generated for each model was reviewed based on the results. The general-purpose program ANSYS was employed to determine the shapes. A multi-linear elasto-plastic model using the von Mises yielding criterion was employed in order to express the elasto-plastic behavior of the film. Figure 3 shows the material constant of the film. With regard to the analytical conditions, the forced displacement condition was assigned to the Z-direction of the arch in the initial plane state considering the initial stress. The analytical scope was set to one-quarter of the whole based on the symmetry of the model.

Figure 4 shows the initial shape of the film by stretching and the stress distribution of the film surface. The analytical results showed that the shape of each model after stretching was similar to the surface with uniform stress, whereas significant stress was generated at the arch and near the arch ends where forced displacement was applied.

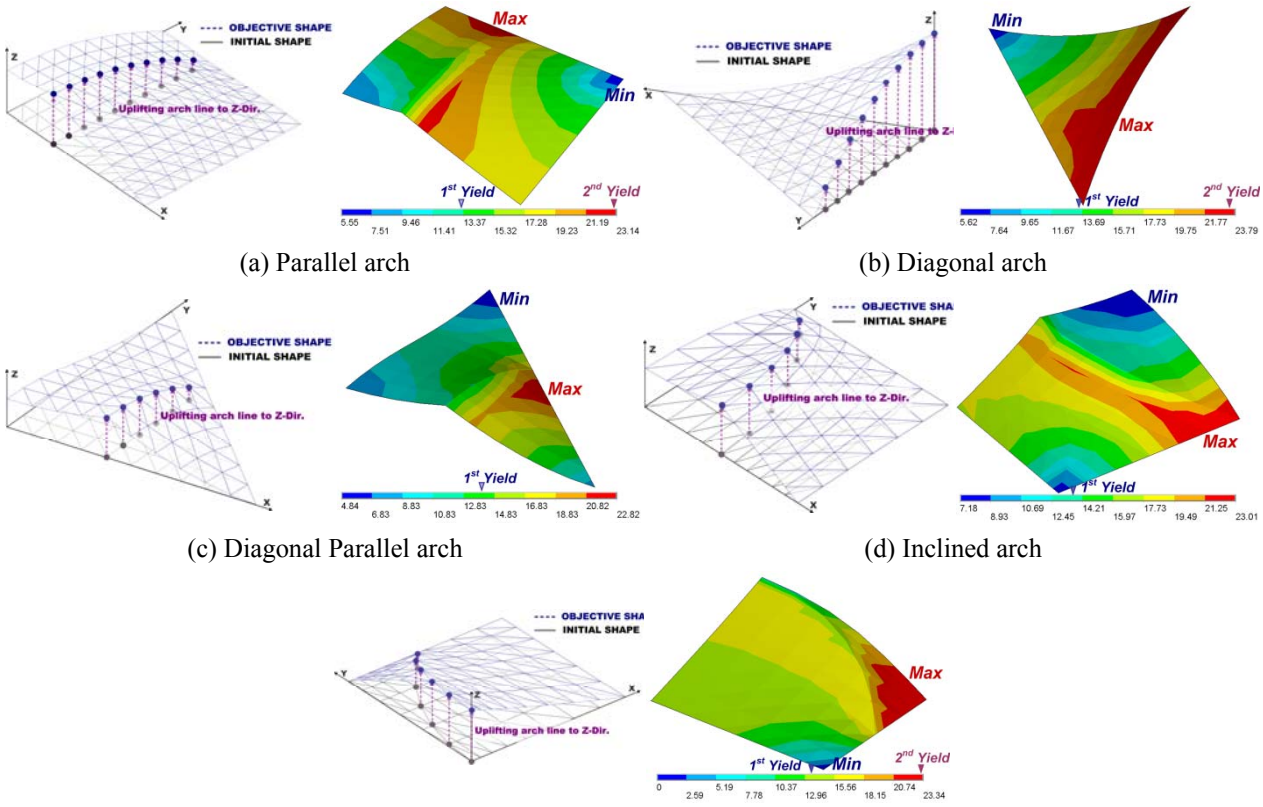

(a) Parallel arch

(b) Diagonal arch

(c) Diagonal Parallel arch

(d) Inclined arch

(e) Cross arch

Figure 4: Initial shape and stress contour by stretch

2.3 Manufacture and investigation of study model

To review the applicability of stretch fabrication, the cutting pattern generated via the method presented in the previous section was used to manufacture each model. Figure 5 shows the manufacturing flow process. Stretch fabrication was conducted by introducing initial stress from the peripheral frame, and the target level of the introduced initial stress was set as the baseline. The reduction rate was considered for the cutting pattern generated by each model in advance. A flat bar was installed on the film after the initial stress was introduced and fastened with a bolt.

Figure 6 shows the results of manufacturing five study models by stretch fabrication. The results confirmed that stretch fabrication can be applied to various shapes fabricated by tensioning and is effective with a cutting pattern generated based on shape. When the initial element area and cutting pattern generation were comparable, the parallel/diagonal parallel/slope/cross arch had almost the same area ratios. Since the error in area ratio was large for the diagonal arch, the result reflected the reduction rate as much as the manufacturing error of the model. In addition, when the initial element area and specimen were compared, the area ratio was greatest at 15% for the diagonal arch and around 5% for the others. Based on the cutting pattern generation, the target level of the area ratio should be set at about 5%.

In real structures, the film becomes thicker, which makes introducing the initial stress from the peripheral frame difficult. Thus, using the arch to introduce the initial stress is more efficient.

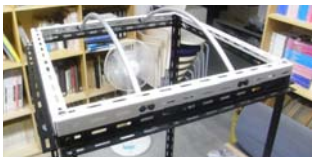
(a) Frame manufacture


(b) Stretch-Fabrication


(c) Fixed by flat bar

Figure 5: Manufacturing flow process


(a) Parallel arch


(b) Diagonal arch


(c) Diagonal parallel arch


(d) Inclined arch


(e) Cross arch

Figure 6: Results of manufacturing five study models by stretch fabrication

3. Mock-up test

3.1 Experimental synopsis

To verify the applicability of stretch fabrication to a real structure, a mock-up test was conducted on the diagonal arch model. In particular, the stress distribution of the film during formation of the curved surface was reviewed, as this had not been clearly analyzed during the manufacture of the study models, along with the dynamic behavior of the film with respect to time after stretch fabrication. The diagonal arch model was chosen so that viscous behavior such as the stress distribution of the film and relaxation could be readily compared and reviewed, and fabrication was easy because of the simple design and symmetric shape. The specimen dimensions were as follows: 200 μm thick ETFE film, square frame made of 1500 mm angles, and two arches with heights of 10% and 15% of the rise span ratio.

3.2 Analytical verification

First, an analytical review was conducted to select the members of the specimen. The general-purpose program ANSYS was employed for shape and stress–strain analyses of the film, whereas MidasGEN was employed for stress analysis of the film. First, the long- (i.e., initial stress) and short-term (i.e., snow, wind) loads of the film were analyzed. To identify the rate that the initial stress was maintained in the real model, analysis was carried out under the hypothetical condition that the load was removed. Figure 7 shows the load conditions.

(a) Long-term load

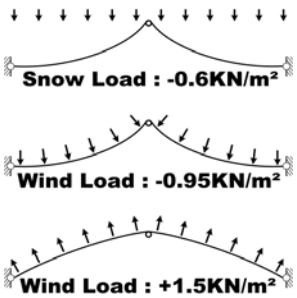

(b) Short-term load

(c) Removing load

Figure 7: Flow of analysis

Figs. 8 and 9 show the short-term load results when the rise span ratios were 10% and 15%, respectively. For the 10% rise span ratio, the maximum stress of the film was in sintering range and exceeded the first yielding point in the broad area around the arch; however, it did not reach the second yielding point. On the other hand, for the 15% rise span ratio, the sintering range was broad compared to that of the 10% rise span ratio; thus, the stress around the arch reached to second yielding point when the initial stress and wind load (i.e., negative pressure) were applied. However, the stress in the corner area perpendicular to the arch became smaller. Figs. 10 and 11 present the stress distributions when the external load was removed.

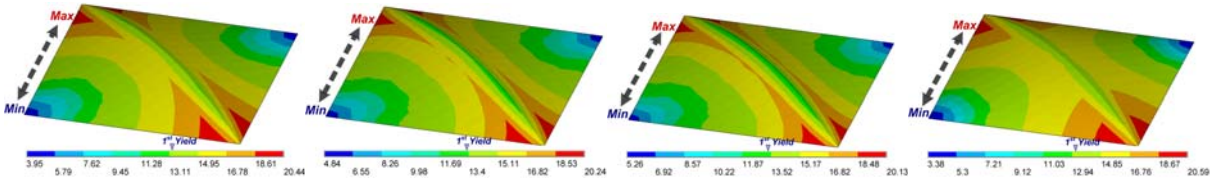

(a) Initial stress (b) Snow load (c) Wind load(downwards) (d) Wind load(uplift)

Figure 8: Initial stress and stress distribution on short-term load(rise-span ratio 10%)

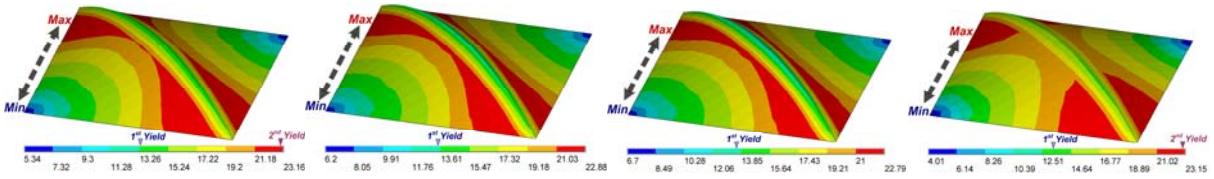

(a) Initial stress (b) Snow load (c) Wind load(downwards) (d) Wind load(uplift)

Figure 9: Initial stress and stress distribution on short-term load(rise-span ratio 15%)

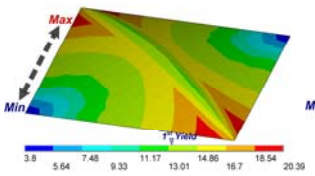

(a) Removing snow load (b) Removing wind load

Figure 10: Stress distribution after removing the external load(rise-span ratio 10%)

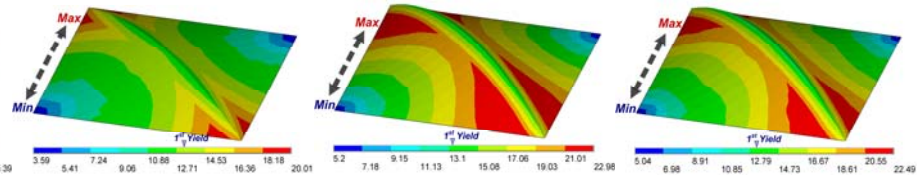

(a) Removing snow load (b) Removing wind load

Figure 11: Stress distribution after removing the external load(rise-span ratio 15%)

Figs. 12 and 13 present the relation between the equivalent stress ($\bar{\sigma}$) and equivalent viscoplastic strain ($\bar{\varepsilon}^{p}$) at rise span ratios of 10% and 15%, respectively. After the initial stress was introduced, the stress increased because of snow and wind loads and decreased after these loads were removed. After the loads were removed, the rate of stress of the film to the initial stress was defined as the maintained stress rate; a 10% rise span ratio maintained 94% of the initial stress against a snow load and 86% against a wind load, whereas a 15% rise span ratio maintained 97% of the initial stress against a snow load and 92% against a wind load.

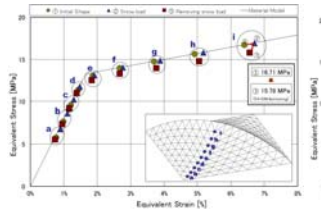

(a) Snow load (b) Wind load(uplift)

Figure 12: Equi. stress-strain relation (Rise 10%)

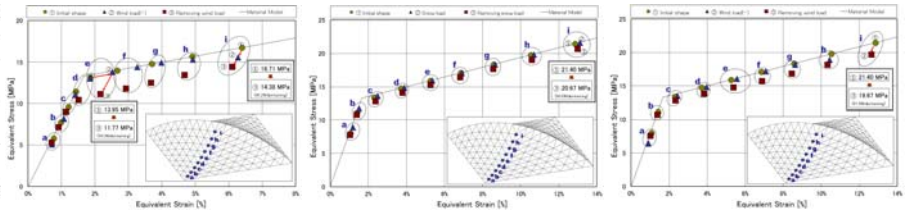

(a) Snow load (b) Wind load(uplift)

Figure 13: Equi. stress-strain relation (Rise 15%)

3.3 Experimental investigation

Figure 14 presents an outline of the specimen. The specimen consisted of a 1.5 m × 1.5 m frame, arch heights of 10% and 15% rise span ratios, and a 200 μm thick ETFE film. The analytical results revealed that a steel section

of 100 mm × 50 mm × 5 mm × 7.5 mm was suitable for the peripheral frame, and a steel pipe with dimensions of φ34 mm × 2.3 mm was suitable for the arch.

The panel-shaped specimen comprised a mounting flat bar and substructure that received the reaction force during stretch fabrication. To identify the stress state of the film during stretch fabrication, we mounted a strain gage at the center and ends of each pillar and arch. From this strain, the reaction force of the pillar and axial force of the arch were calculated for comparison with the analysis. Grid lines were drawn on the film in advance. The strain before and after stretch fabrication and the remaining strain were then measured. The stretch fabrication procedure is ; first, a film was attached to a frame. The arch for stretch fabrication was fastened to a pillar. The frame was passed through the bar installed at each pillar, and then the frame was raised and lowered with a bolt to induce stress. The frame descended in increments of 2 mm at uniform time intervals.

Figures 15 and 16 present the test conditions. Raising the arch allowed the film to be stretched in a stable manner. However, after termination of the test, significant deformation in the frame of the specimen with the 15% rise span ratio occurred because of the initial stress of the film at the corner orthogonal to the arch, and it could not be removed from the pillar.

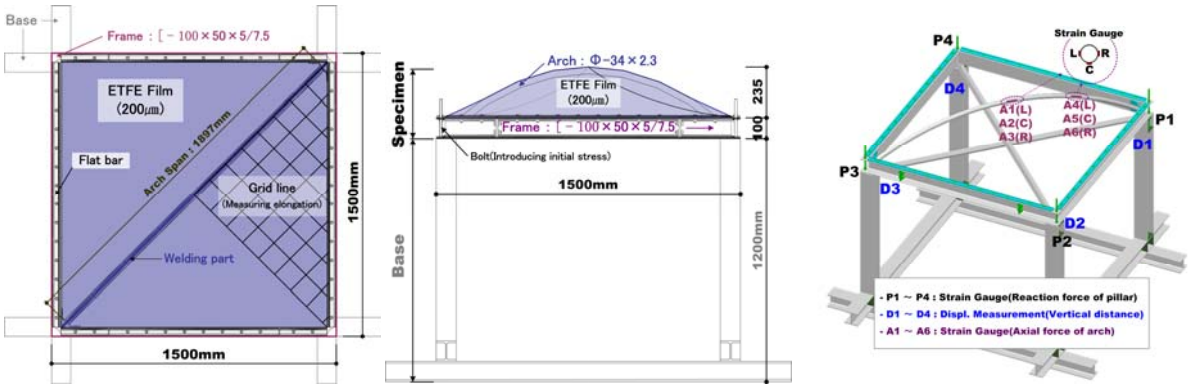

(a) Plan (b) Section (d) Measuring position

Figure 14: Outline of specimen

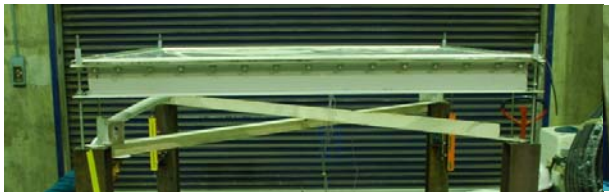

(a) Before stretch fabrication

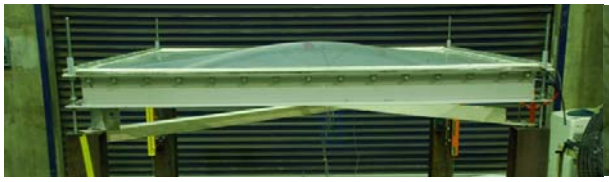

(b) During stretch fabrication

(c) After stretch fabrication

Figure 15: Configuration of stretch fabrication(rise 10%)

(a) Before stretch fabrication

(b) During stretch fabrication

(c) After stretch fabrication

Figure 16: Configuration of stretch fabrication(rise 15%)

3.4 Comparison of results of analysis and experiment

Figures 17 and 18 present the relation between the vertical displacement of the frame and the axial force of the center and ends of the arch. The experimental and analytical results were found to coincide in both cases, which led to the hypothesis that phenomena observed in the tests could be reproduced in the analysis.

Figures 19 and 20 show the axial force of the arch and temperature change with respect to elapsed time in the test. After stretch fabrication was completed, the axial force of the arch decreased and then started to increase after 20 min. Then, the axial force showed almost the same behavior as the temperature change. Based on these results, film relaxation occurred 20 min after stretch fabrication but became negligible after that.

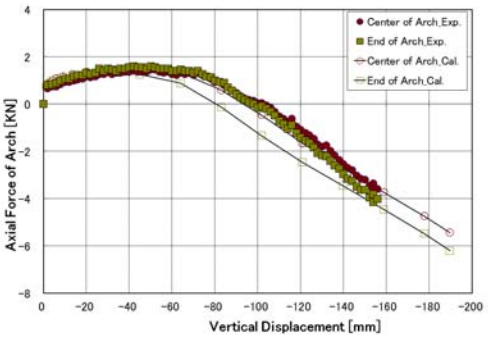

Figure 17: Verti. displacement & axial force relation (rise span ratio10%)

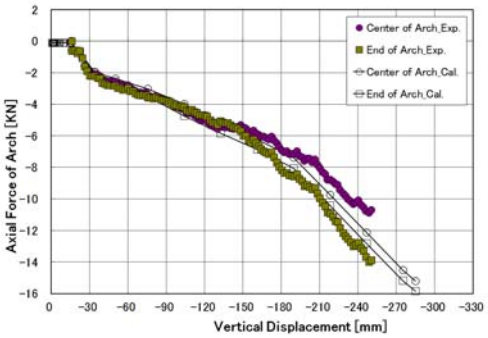

Figure 18: Verti. displacement & axial force relation (rise span ratio15%)

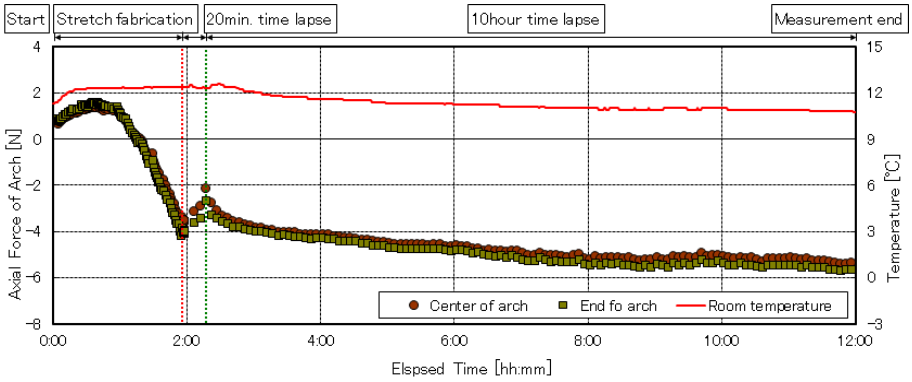

Figure 19: Relation between the axial force and temperature change on elapsed time(rise span ratio 10%)

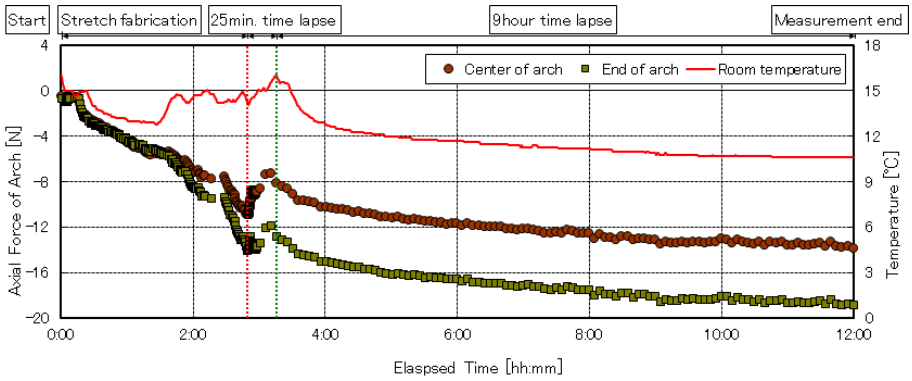

Figure 20: Relation between the axial force and temperature change on elapsed time(rise span ratio 15%)

4. Conclusion

In this study, we reviewed the applicability of stretch fabrication to study models and actual-size models using ETFE film and drew the following conclusions.

By manufacturing a study model and performing tests, we were able to verify that stretch fabrication can be applied to films with various shapes and is an effective method for making film with high strength.

Stretch fabrication was found to be more efficient when the initial stress was introduced with the arch rather than the peripheral frame.

The verification tests confirmed that the change in axial force of the arch showed almost the same behavior as the analytical results, which confirmed the effectiveness of elasto-plastic analysis.

For the axial change in the arch with respect to time, we confirmed that after stretch fabrication, the compressive force increased after tensile force was produced; this was caused by temperature change rather than film relaxation.

References

[1] Kawabata M. and Jeong E.S., Study on Three Dimensional Fabrication of ETFE Film Panel by Stretching-Part 1:Outline of Fabrication by Stretching, Summaries of Technical Papers of Annual Meeting Architectural Institute of Japan, 2008, 931-932(in Japanese)

[2] Kawabata M., Jeong E.S. and Okamura U., A study on Film Membrane Structures with Stress Introduction by Stretching Boundaries Part 1, Part 2 and Part 3, Summaries of Technical Papers of Annual Meeting Architectural Institute of Japan, 2012, 919-922(in Japanese)

[3] Moriyama F., Kawabata M. and Masaki K., Elasto-plastic characteristic of ETFE film, Research Report on Membrane Structures, 2004; **17**; 21-26(in Japanese)

[4] Yoshino T., Segawa S. and Oda K., Material Characteristics of ETFE Film Under The Biaxial Tension, Research Report on Membrane Structures, 2005; **18**; 31-39(in Japanese)

[5] Kawabata M. and Moriyama F., Study on Strain Velocity Dependency and Structural Characteristics of ETFE films, Research Report on Membrane Structures, 2005; **18**; 41-46(in Japanese)

[6] Kawabata M., Moriyama F. and Aida H., Viscoelastic characteristic of ETFE film, Research Report on Membrane Structures, 2006; **19**; 31-39(in Japanese)

[7] Malinin N. N., Khadjinsky G. M., Theory of Creep with Anisotropic Hardening, Int. J. Mech. Sci., 1972; **14**; 235-246.

[8] The Japan Society of Material Science, Elements of Solid Mechanics, Nikkan Kogyo Shimbun Ltd., Japan, 1981(in Japanese)

[9] Armstrong P. J., Frederick C. O., DEGB Rep., No.RD/B/N731, 1966.

[10] Sanomura Y., Mizuno M., Viscoplastic Constitutive Equation of High-Density Polyethylene", Jpn. Soc. Mech. Eng., 2004; **38**; 7-13(in Japanese)

[11] Design and Guideline of ETFE Film Panel, Membrane Structures Association of Japan, 2006(in Japanese)

[12] Roesler J., Handers H. and Baeker M., Mechanical Behavior of Engeering Materials-Metals, Ceramics, Polymers and Composites, Springer, 2007.

[13] L. E. Nielsen, Mechanical Properties of Polymers and Composites, Marcel Dekker, USA, 1994